MOLECULAR AND CELLULAR BIOLOGY, Mar. 2006, p. 2065–2079 Vol. 26, No. 6
0270-7306/06/$08.00+0 doi:10.1128/MCB.26.6.2065–2079.2006

PB1 Domain-Dependent Signaling Complex Is Required for Extracellular Signal-Regulated Kinase 5 Activation

Kazuhiro Nakamura, Mark T. Uhlik, Nancy L. Johnson, Klaus M. Hahn, and Gary L. Johnson*

Department of Pharmacology and Lineberger Comprehensive Cancer Center, University of North Carolina School of Medicine, Chapel Hill, North Carolina 27599-7365

Received 28 October 2005/Returned for modification 22 November 2005/Accepted 22 December 2005

MEKK2, MEK5, and extracellular signal-regulated kinase 5 (ERK5) are members of a three-kinase cascade for the activation of ERK5. MEK5 is the only MAP2K to express a PB1 domain, and we have shown that it heterodimerizes with the PB1 domain of MEKK2. Here we demonstrate the MEK5 PB1 domain is a scaffold that also binds ERK5, functionally forming a MEKK2-MEK5-ERK5 complex. Reconstitution assays and CFP/YFP imaging (fluorescence resonance energy transfer [FRET]) measuring YFP-MEKK2/CFP-MEK5 and CFP-MEK5/YFP-ERK5 interactions define distinct MEK5 PB1 domain binding sites for MEKK2 and ERK5, with a C-terminal extension of the PB1 domain contributing to ERK5 binding. Stimulus-dependent CFP/YFP FRET in combination with mutational analysis was used to define MEK5 PB1 domain residues critical for the interaction of MEKK2/MEK5 and MEK5/ERK5 required for activation of the ERK5 pathway in living cells. Fusion of the MEK5 PB1 domain to the N terminus of MEK1 confers ERK5 regulation by a MAP2K normally regulating only ERK1/2. The MEK5 PB1 domain confers stringent MAP3K regulation of ERK5 relative to more promiscuous MAP3K control of ERK1/2, JNK, and p38.

Extracellular signal-regulated kinase 5 (ERK5), also referred to as BMK1, is a mitogen-activated protein kinase (MAPK) activated by a variety of growth factors and stress stimuli (9). ERK5 appears to be expressed in most tissues of adult mice and humans (16). To date, defined targets for ERK5 include connexin 43 (2), Rsk (20), and the transcription factors MEF2A, -C, and -D (13); Sap1a (12); SGK (10); and PPARγ1 (1). Targeted gene disruption of ERK5 is embryonic lethal due to defects in cardiac development and angiogenesis (22, 24, 32). Constitutive activation of ERK5 in the heart of a transgenic mouse expressing an activated mutant of MEK5, the MAPK kinase that phosphorylates and activates ERK5, leads to cardiac hypertrophy and death of the animal at approximately eight weeks of age (18). ERK5 is also important in neuronal survival (8, 30) and appears to play a critical role in protecting many cell types from stress-induced apoptosis (14).

Like other MAPKs, ERK5 is part of a three-kinase module, which for ERK5 involves MEK5 (the MAP2K) and MEKK2 or MEKK3 (the MAP3Ks) (5, 34). MEK5, MEKK2, and MEKK3 are the only MAP2K and MAP3Ks that encode Phox/Bem1p (PB1) domains. Heterodimers of MEKK2 or MEKK3 with MEK5 are formed via interaction between their respective PB1 domains, which confers a selectivity for ERK5 activation by MEKK2 and MEKK3 and not other MAP3Ks (17). Thus, PB1 domain-dependent MEKK2/3-MEK5 heterodimers provide a spatially organized signaling complex primed to activate ERK5 in response to activation of MEKK2 or MEKK3.

PB1 domains (21) form heterodimers using a β grasp topology in a "front-to-back" arrangement (27, 31). In this configuration, clusters of basic amino acids in the front of one PB1 domain interact with clusters of acidic amino acids in the back of a second PB1 domain (15). MEKK2 and MEKK3 have atypical PB1 domains which lack key residues in the acidic cluster. We show that PB1 domains of MEKK2 and MEKK3, therefore, use the front basic cluster to bind to the MEK5 rear end acidic cluster.

We also demonstrate here the function of the PB1 domain of MEK5 in forming a functional MEKK2-MEK5-ERK5 signaling complex. We have used YFP-MEKK2, CFP-MEK5, and YFP-ERK5 as biosensors to assay the behavior of MEK5 interactions with MEKK2 and ERK5 using fluorescence resonance energy transfer (FRET)-based live cell assays in combination with coimmunoprecipitation and in vitro reconstitution of protein complexes. The present study describes a previously undefined function of PB1 domains for the stringent control of ERK5 activation that is unique for ERK5 and not observed with the control of other MAPKs.

MATERIALS AND METHODS

Three-dimensional modeling of PB1 domains. Models of PB1 domains from MEKK2 (amino acids 43 to 122) and MEK5 (amino acids 16 to 109) were built by using the Modeler module of the InsightII molecular modeling system from Accelrys, Inc., using nuclear magnetic resonance solution structures of Bem1p PB1 (1IP9) and Cdc24p PB1 (1Q10) domains, respectively, as templates (27).

Live cell FRET microscopy and image analysis. For live cell CYFRET experiments, COS7 cells were transfected on 25-mm round glass coverslips. After 24 to 48 h, cells were placed in an imaging chamber at room temperature in media. CYFRET image acquisition and analysis were conducted by the three-filter micro-FRET image subtraction methods (19, 29). Briefly, three images (100-ms exposure, 2 × 2 binning) were obtained: yellow fluorescence protein (YFP) excitation/YFP emission, cyan fluorescence protein (CFP) excitation/CFP emission, and CFP excitation/YFP emission (raw, uncorrected CYFRET). Background-subtracted YFP and CFP images were fractionally subtracted from background-subtracted uncorrected CYFRET images on the basis of measurements for CFP bleedthrough (0.49 to 0.54) and YFP cross-excitation (0.019-0.022). This fractional subtraction procedure generated corrected FRET ($FRET^c$) images, which were utilized to create representative visual images in monochrome, show-

* Corresponding author. Mailing address: Department of Pharmacology, CB#7365, 1108 Mary Ellen Jones Building, University of North Carolina at Chapel Hill, Chapel Hill, NC 27599-7365. Phone: (919) 843-3107. Fax: (919) 966-5640. E-mail: gary_Johnson@med.unc.edu.

ing sensitized FRET within the cells. For data analysis, FRETN^c (FRET^c/[CFP × YFP]) or FRET^c/CFP (FRET^c divided by CFP) was used to normalize all FRET values. The data were analyzed for statistical significance by using a paired Student *t* test.

Imaging was conducted by using a Zeiss Axiovert 200M inverted microscope with a 125-W xenon arc lamp (Sutter Instrument Company, Novato, CA), digital charge-coupled device camera (CoolSNAP HQ; Roper Scientific, Tucson, AZ), and Slidebook 4.0.10 software (Intelligent Imaging Innovations, Denver, CO). An objective lens (63× oil 1.25-numerical aperture, Plan-Neofluar [Zeiss]) was coupled with immersion oil to the bottom face of glass coverslips. Three images (CFP [a band-pass excitation filter of 436/20 nm, a 455DCLP band beamsplitter, and a band-pass emission filter of 480/40 nm], YFP [a band-pass excitation filter of 500/20 nm, a 515DCLP band beamsplitter, and a band-pass emission filter of 535/30 nm], and FRET [a band-pass excitation filter of 436/20 nm, a JP4 86002 multiband beamsplitter, and a band-pass emission filter of 535/30 nm]; Chroma) were obtained at 100-ms exposure 2 × 2 binning by using the multipoint setup function.

Pull-down assays with GST fusion proteins. The different glutathione *S*-transferase (GST) fusion proteins were coupled to glutathione beads. His/Xpress tagged protein was purified with nickel-nitrilotriacetic acid columns. Total cell lysates were prepared from HEK293 cells transiently transfected with FLAG-MEK5, hemagglutinin (HA)-MEKK2, HA-MEKK3, and Xpress-ERK5 by using a solubilizing buffer described below. GST fusion proteins on glutathione beads were incubated with 5 μg of purified His/Xpress-tagged protein in 1% Triton X-100–phosphate-buffered saline or 1 mg of HEK293 cell lysate at 4°C for 2 h. The beads were washed five times with solubilizing buffer. The protein complex isolated on the beads was subjected to sodium dodecyl sulfate-polyacrylamide gel electrophoresis (SDS-PAGE) and immunoblotting for analysis.

Immunoprecipitation and immunoblotting analysis. Cells were washed three times with ice-cold phosphate-buffered saline and lysed with solubilizing buffer (1% NP-40, 10 mM Tris [pH 7.5], 150 mM NaCl, 0.4 mM EDTA, 10 mM NaF, 2 mM Na_3VO_4, 1 μg of leupeptin/ml, 1 μg of aprotinin/ml, 1 μg of α_1-antitrypsin/ml, and 1 mM phenylmethylsulfonyl fluoride), and cleared supernatants were retained for further processing. Lysates were subjected to immunoblotting or immunoprecipitation with anti-FLAG or anti-MEKK2 monoclonal antibody. For immunoprecipitation, immune complexes were collected with protein G-Sepharose beads, separated by SDS-PAGE, and transferred to a nitrocellulose membrane. After blocking, membranes were blotted with the indicated antibodies and visualized by using the Supersignal West Pico detection system.

RESULTS

MEK5 PB1 domain contributes to ERK5 binding. MEK5 is a 448-amino-acid protein with the PB1 domain encoded by residues 18 to 97 and the kinase domain within residues 166 to 448. A GST fusion of MEK5 residues 18 to 165 (Δkinase MEK5) that includes the PB1 domain, but not the kinase domain binds ERK5 (Fig. 1A). The PB1 domain (residues 18 to 97) alone or the sequence encoded by residues 98 to 165 C terminal to the PB1 domain both fail to bind ERK5. Figure 1B shows coimmunoprecipitation of full-length or Δkinase MEK5 with ERK5. Full-length MEK5 and the N-terminal Δkinase MEK5 domain both bind ERK5. The findings show that the MEK5 PB1 domain and a sequence C terminal to the PB1 domain are involved in binding ERK5. Coexpression of MEKK2, ERK5, and different peptide sequences of MEK5 further show that the N terminus of MEK5 is capable of forming a ternary complex with MEKK2 and ERK5 (Fig. 1C). Antibodies specific for MEKK2 are able to coimmunoprecipitate ERK5 when full-length or the N-terminal Δkinase domain of MEK5 is expressed. Furthermore, mutation of the MEK5 T loop residues ^{311}S and ^{315}T to A and V (^{311}S^{315}T-AV MEK5), respectively, to inhibit MEK5 activation has no influence on formation of the ternary complex. Cumulatively, the findings indicate that the N terminus of MEK5 functions to bind both MEKK2 and ERK5. The N-terminal MEK5 sequence (amino acids 18 to 165) that binds ERK5 does not bind p38, JNK, or ERK1, demonstrating that this sequence uniquely binds ERK5 but not other MAPKs (Fig. 1D).

Figure 2 further refines the region of the MEK5 N terminus that binds ERK5 and MEKK2. The MEK5 PB1 domain (amino acids 18 to 97) is sufficient to bind MEKK2 but not ERK5. ERK5 binding requires an intact PB1 domain and an extension of residues immediately downstream of the PB1 domain. In contrast, the N-terminal moiety of the MEK5 PB1 domain is not required for MEKK2 binding; only the C-terminal moiety starting at amino acid 56 of the MEK5 PB1 domain is required for MEKK2 binding (Fig. 2A and B). Kinase inactive MEKK2 (^{385}K-M MEKK2) binds MEK5 (Fig. 2A and C) similar to wild-type (WT) MEKK2 (Fig. 1), a finding consistent with scaffolding functions for MEKK2-MEK5 binding independent of the kinase domain. In contrast, a MEKK2 PB1 domain mutation at a conserved lysine residue (^{47}K-A [see below]) causes loss of MEK5 binding (Fig. 2A and C). The shortest N-terminal MEK5 fragment that binds ERK5 includes the PB1 domain (residues 18 to 97) and 34 additional residues C terminal to the PB1 domain (residues 98 to 131) (Fig. 2C and D). Mutation of residues ^{20}R^{21}I to alanines within the MEK5 PB1 domain causes loss of ERK5 binding but not MEKK2 binding (Fig. 2E). In contrast, MEKK2 binds to the C-terminal moiety of the MEK5 PB1 domain (amino acids 56 to 97) independent of the C-terminal extension (Fig. 2A and C and Fig. 4D). Thus, mutation analysis distinguishes between residues required for ERK5 and MEKK2 binding within the PB1 domain.

Structural model for MEKK2-MEK5 PB1 domain interaction. The PB1 domain is found in a small number of proteins in yeast, plants, and metazoans (21). Figure 3A shows the sequence alignment for the PB1 domains of several proteins, including MEK5, MEKK2, and MEKK3; MEKK2 and MEKK3 are highly conserved MAP3Ks that regulate the ERK5 pathway. PB1 domains consist of two α helices and a five-stranded β sheet (11, 31). Near the N-terminal region of the PB1 domain there is a conserved lysine or arginine corresponding to ^{22}K in MEK5, ^{47}K in MEKK2, and ^{48}K in MEKK3. The C-terminal region of the MEK5 PB1 domain encodes an OPCA motif that contains a conserved acidic amino acid cluster starting at ^{64}D. The acidic cluster is markedly altered in MEKK2 and MEKK3, with asparagines replacing the corresponding ^{64}D and ^{65}E residues in MEK5. Based on our previous work characterizing the MEKK2-MEK5 PB1 domain interaction (17), we modeled the three-dimensional structure of the MEKK2-MEK5 PB1 domain heterodimer by using the crystal structure of the p40^{phox} and p67^{phox} PB1 domain complex (31) (Fig. 3B). The binding interface of MEKK2 and MEK5 is predicted to involve ^{47}K of MEKK2 and the acidic cluster of MEK5 starting with residues ^{64}D^{65}E. The conserved lysine (^{22}K) in MEK5 is predicted to be on the back side of acidic residues within the OPCA motif. The β4 strand and β4/α2 loop region divides the OPCA motif into two acidic clusters: AC1 in the β3/β4 loop and AC2 at the N terminus of α helix 2. Our model predicts that the first acidic cluster (AC1) of the MEK5 PB1 domain plays a crucial role in interacting with ^{47}K of MEKK2. To test this model, alanine substitutions were introduced within the MEK5 PB1 domain at ^{22}K and at ^{64}D^{65}E and ^{67}G^{68}D in the β3/β4 loop (AC1) and at ^{75}D^{76}E at the N-terminal end of α helix 2 (AC2). The different MEK5 proteins were examined for their interaction with MEKK2 and MEKK3. In addition, the conserved lysine (^{47}K)

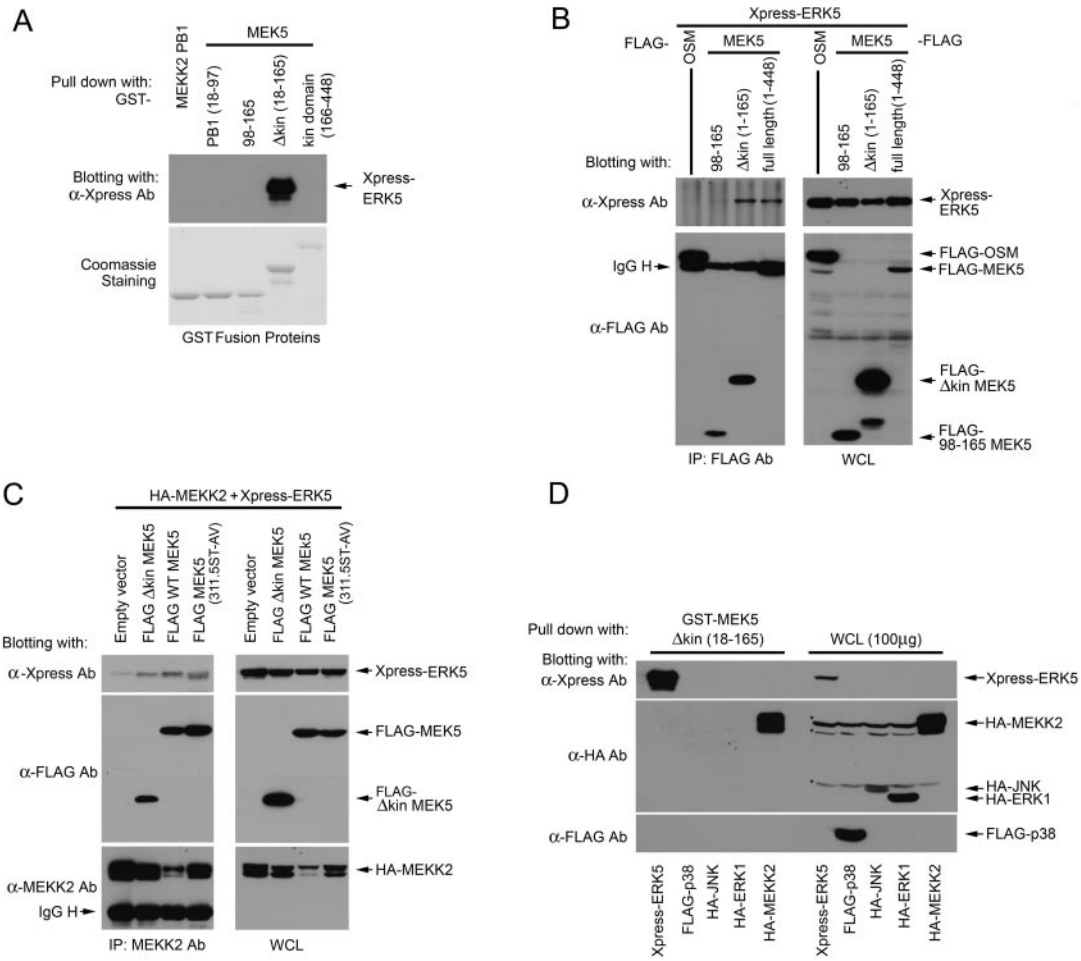

FIG. 1. PB1 domain-dependent interaction of MEK5 and ERK5. (A) The indicated MEK5 GST fusion proteins were tested for their ability to bind ERK5. Xpress-ERK5 from HEK293 cell lysates was used in pull-down assays using GST fusions of the MEK5 PB1 domain (residues 18 to 97), MEK5 residues 98 to 165, MEK5 residues 18 to 165 lacking the kinase domain (Δkinase), the MEK5 kinase domain (residues 166 to 448), or a control using the MEKK2 PB1 domain. Adsorbents were resolved by SDS-PAGE and immunoblotted with anti-Xpress antibody. The amount of GST fusion protein used in each assay is shown by Coomassie blue staining (bottom panel). (B) In vivo binding of MEK5 protein sequences and ERK5. Full-length Xpress-ERK5 was expressed with FLAG-MEK5 deletion constructs. OSM (for osomsensing scaffold for MEKK3), which does not bind MEK5, was used as a control. FLAG-proteins were immunoprecipitated with anti-FLAG antibody. The adsorbents were analyzed by immunoblotting with anti-Xpress or anti-FLAG antibody (left panel). The expression of each protein was confirmed by immunoblotting of whole-cell lysates (right panel). (C) Demonstration of a MEKK2-MEK5-ERK5 ternary complex in cells. FLAG-tagged WT, Δkinase, and ^{311}S^{315}T-AV MEK5 ($^{311.5}$ST-AV in the figure) proteins were expressed with HA-tagged MEKK2 and Xpress-tagged ERK5. HA-tagged MEKK2 was immunoprecipitated with anti-MEKK2 antibody, and the immunocomplexes were analyzed by using anti-Xpress (for ERK5) and anti-FLAG (for MEK5) antibody immunoblots (left panel). The expression of each protein was confirmed by anti-MEKK2, anti-FLAG, and anti-Xpress antibody immunoblotting of whole-cell lysates (right panel). (D) Specificity of the MEK5 Δkinase(18-165) protein interaction with MAPKs. Xpress-ERK5, FLAG-p38, HA-JNK, HA-ERK1, or HA-MEKK2 were tested for binding of the GST-MEK5 Δkinase(18-165) fusion protein. The adsorbents were resolved and sequentially immunoblotted with anti-Xpress (for ERK5), anti-FLAG (for p38), and anti-HA (MEKK2, JNK, and ERK1) antibodies (left panel). Protein expression for each construct is shown by blotting of whole-cell lysates (right panel). Nonspecific bands in the anti-HA blots are marked with an asterisk.

was mutated to alanine in MEKK2 for analysis of MEK5-MEKK2 interactions.

MEKK2-MEK5 interaction. To analyze the requirements of PB1 domains for MEK5-MEKK2 and MEK5-MEKK3 interactions, a GST fusion of the MEKK2 or MEKK3 PB1 domain was used in pull down assays of Xpress/His-tagged WT or mutant MEK5 PB1 domains (Fig. 3C). MEKK2 and MEKK3 PB1 domains similarly bound the WT and ^{22}K-A MEK5 PB1 domains, indicating the conserved lysine at the front end of the MEK5 PB1 domain was not required for binding to the MEKK2 or MEKK3 PB1 domain. In contrast, two different AC1 mutations (^{64}D^{65}E-AA and ^{67}G^{68}D-AA) abolished MEKK2 or MEKK3 PB1 domain binding. Mutation of ^{75}D^{76}E-AA had little or no effect on MEKK2 and a partial inhibition of MEKK3 PB1 domain binding. Mutation of the conserved lysine in both MEKK2 (^{47}K-A) and MEKK3 (^{48}K-A) PB1 domains caused the complete loss of binding to the MEK5 PB1 domain (Fig. 3C, right panels). Thus, the heterodimerization of MEK5-MEKK2 and MEK5-MEKK3 PB1 domains require the conserved lysine in MEKK2 or MEKK3 and residues in the first acidic cluster (AC1) of MEK5.

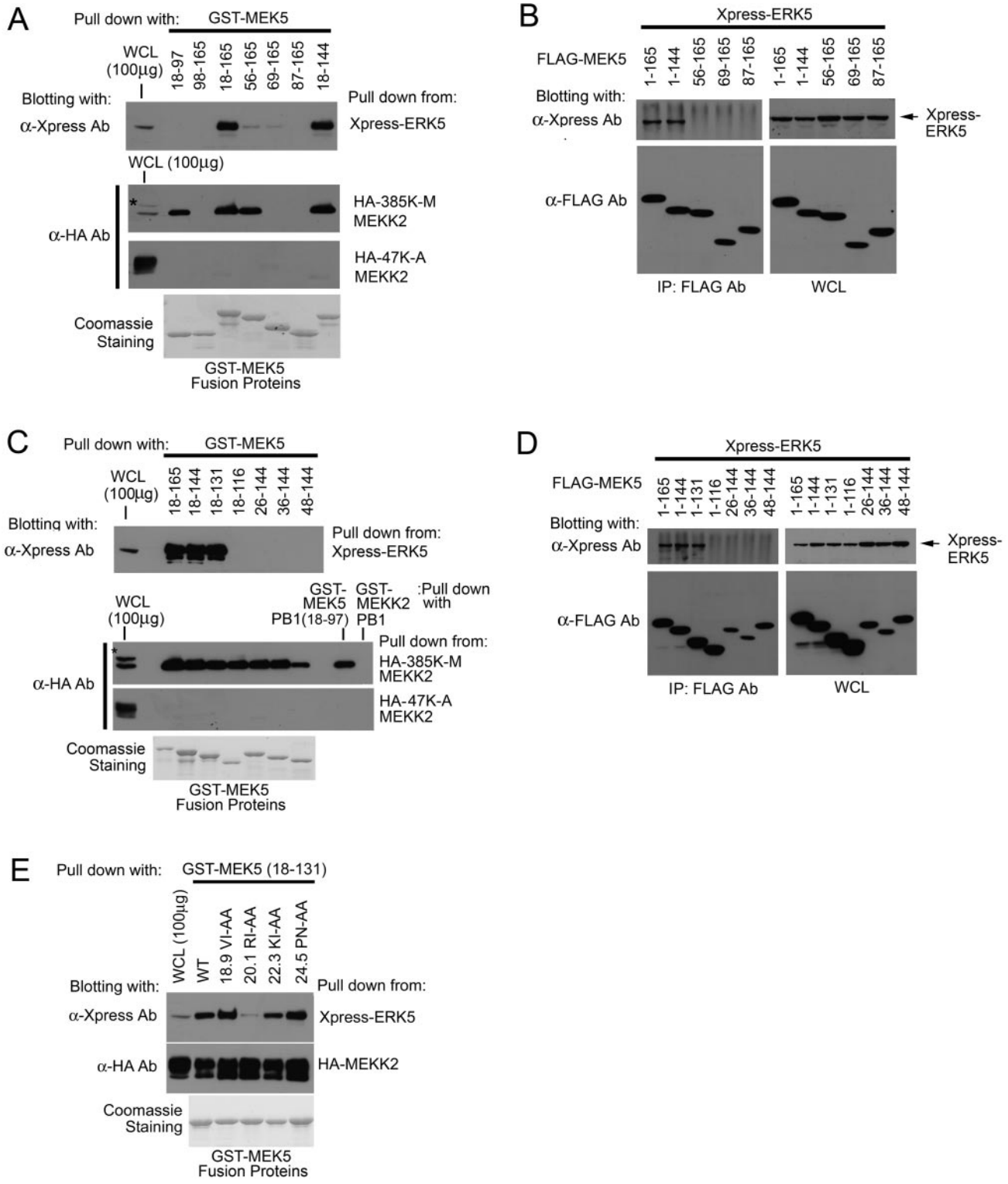

FIG. 2. Mapping of the ERK5 binding site in MEK5. (A) ERK5 and MEKK2 binding sites in MEK5 were analyzed by using MEK5 deletion mutants. GST fusion proteins of the indicated MEK5 fragments (amino acids 18 to 97, etc.) were used to analyze binding to full-length WT ERK5, kinase-inactive MEKK2 (^{385}K-M), and the ^{47}K-A PB1 domain MEKK2 mutant proteins. The adsorbents and 100 μg (10% of the lysates used for pull down assay) of each whole-cell lysate were analyzed with anti-Xpress (for ERK5) or anti-HA (for MEKK2) blotting. A nonspecific band in the anti-HA blot is marked with an asterisk. The bottom panel shows the expression of GST fusion proteins used in the assay. (B) Binding in cells of full-length ERK5 to different MEK5 sequences that encode the indicated amino acid sequences (1 to 165, etc.). FLAG-tagged deletion mutants of MEK5 were coexpressed with Xpress-ERK5 and immunoprecipitated with anti-FLAG antibody. ERK5 binding was detected by anti-Xpress antibody blotting of the immunoprecipitates (left panel). The expression of each protein was determined by immunoblotting of whole-cell lysates (right panel). The mobility of FLAG-MEK5 69-165 and 87-165 deletion constructs is anomalous presumably due to the deletion of negatively

Interactions defined between PB1 domains are the same for full-length proteins (Fig. 3D). Both MEKK2 and MEKK3 PB1 domains bound WT and ^{22}K-A mutated full-length MEK5 but not ^{64}D^{65}E-AA or ^{67}G^{68}D-AA MEK5 mutant protein, and functional MEKK2 and MEKK3 PB1 domains are required for full-length MEK5 coimmunoprecipitation with full-length MEKK2 (Fig. 3E). Neither the ^{64}D^{65}E-AA nor the ^{67}G^{68}D-AA mutant MEK5 proteins interacted with MEKK2. The ^{75}D^{76}E-AA mutant MEK5 protein bound MEKK2 less efficiently than WT MEK5 (Fig. 3E), a finding similar to that observed with isolated PB1 domains (Fig. 3D). The MEKK2 interaction with ^{22}K-A mutated MEK5 was similar to WT MEK5. These findings indicate that the C-terminal moiety of the MEK5 PB1 domain is critical for binding the MEKK2 or MEKK3 PB1 domain. To prove this, GST fusions of the full-length (residues 18 to 97) or C-terminal moiety (residues 56 to 97) of the MEK5 PB1 domain were used to pull down MEKK2 (Fig. 3F). Both fusion proteins equally bound MEKK2. In contrast, mutation of the acidic cluster in the C-terminal fragment of the MEK5 PB1 domain inhibited MEKK2 binding. These findings and data in Fig. 2 demonstrate that within PB1 domains it is the acidic cluster (^{64}D^{65}E, ^{67}G^{68}D) in the C-terminal moiety of MEK5 and the conserved lysine in the N-terminal moiety of MEKK2 (^{47}K) and MEKK3 (^{48}K) that are critical for stable MEK5-MEKK2 and MEK5-MEKK3 heterodimerization.

Our goal is to define the behavior of MAPK signaling complexes in single living cells. Therefore, we used FRET microscopy to visualize the interactions of WT and mutant MEKK2 and MEK5. To analyze MEKK2-MEK5 interaction in cells, we used the technique of micro-FRET, where corrected FRET (FRET^c) was calculated pixel by pixel after digital images from single cells through CFP, YFP, and FRET channels were acquired (19, 29). Figure 3G shows FRET^c images created using the micro-FRET subtraction algorithm when WT and mutant forms of the two kinases were coexpressed as CFP-MEK5 and YFP-MEKK2 proteins. YFP-MEKK2 and CFP-MEK5 show a high level of interaction, as depicted by robust FRET^c images (Fig. 3G). Multiple cells were then analyzed for FRET^c to compare normalized FRET^c (FRETN^c) values (Fig. 3H). Cells expressing WT full-length MEKK2 and MEK5 had FRETN^c values of $(6.02 \pm 0.61) \times 10^{-5}$. Cells expressing only YFP-MEKK2 or CFP-MEK5 gave no FRET^c, and control cells expressing YFP-MEKK2 and CFP alone gave FRETN^c values of $(1.33 \pm 0.97) \times 10^{-5}$ (data not shown), indicating the specificity of our FRET^c measurements for the interaction of YFP-MEKK2 and CFP-MEK5.

The significant FRET^c values measured with the interaction of YFP-MEKK2 and CFP-MEK5 allowed direct living cell measurement of the effect of PB1 domain mutations on MEKK2-MEK5 complexes (Fig. 3G and H). Cells expressing MEK5 harboring the ^{64}D^{65}E-AA PB1 domain mutation no longer interacted with MEKK2 [FRETN^c value of $(0.41 \pm 0.33) \times 10^{-5}$ versus $(6.02 \pm 0.61) \times 10^{-5}$ for WT MEK5]. Although the ^{22}K-A MEK5 PB1 domain mutation had no effect on MEKK2-MEK5 interaction [FRETN^c $(6.39 \pm 1.93) \times 10^{-5}$], mutation of the conserved lysine to alanine (^{47}K-A) in the PB1 domain of MEKK2 inhibited MEK5-MEKK2 interaction in cells [FRETN^c $(1.11 \pm 0.89) \times 10^{-5}$]. Deletion of either the MEKK2 or MEK5 PB1 domain also abolished the interaction of MEKK2 and MEK5. Mutation of the MEK5 T-loop phosphorylation sites (^{311}S^{315}T-AV MEK5) had no effect on the interaction of MEKK2 and MEK5, indicating that phosphorylation or activation of MEK5 is not needed for MEKK2-MEK5 interaction. To further prove that the FRET^c changes resulted from altered interaction of the PB1 domains, similar experiments were done with isolated PB1 domains. WT and mutant forms of YFP-MEKK2 and CFP-MEK5 PB1 domains were coexpressed and analyzed for FRETN^c (data not shown). Consistent with the results using the full-length kinases, WT PB1 domains give strong FRETN^c, whereas the ^{47}K-A MEKK2 mutation and ^{64}D^{65}E-AA MEK5 mutant have FRETN^c values reduced to background levels. The findings demonstrate that interaction of MEKK2 and MEK5 in cells requires that both proteins have functional PB1 domains. Thus, the PB1 domains of MEKK2 and MEK5 form heterodimers of the two kinases that are readily detected in cells by CFP-YFP FRET. Our results demonstrate the ability to use micro-FRET to study the interaction of a MAP3K and MAP2K in single living cells.

PB1 domain requirements for the MEKK2-MEK5-ERK5 ternary complex. A functional PB1 domain interaction between MEKK2 and MEK5 is required for the association of ERK5 in MEKK2 complexes. Figure 4A and B shows that mutation of MEK5 residues ^{64}D^{65}E to alanines causes loss of MEKK2 binding but not ERK5 binding. The ^{64}D^{65}E-AA mutations in the MEK5 PB1 domain inhibit MEKK2-MEK5 heterodimerization and the coimmunoprecipitation of ERK5 in MEKK2 immunoprecipitates (Fig. 4C). Figure 4D shows the cumulative mapping studies defining the MEK5 binding properties for MEKK2 and ERK5. The findings are provocative for several reasons. First, to bind MEK5, ERK5 clearly requires a full-length MEK5 PB1 domain (amino acids 18 to 97) initially defined as a binding domain for MEKK2. In contrast, MEKK2 only requires the MEK5 C-terminal moiety of the PB1 domain, including acidic cluster 1, a finding consistent with the loss of binding with the ^{64}D^{65}E-AA mutation within acidic cluster 1. Thus, MEKK2 and ERK5 both use the PB1 domain of MEK5 for binding; beyond the PB1 domain of MEK5, an additional sequence from amino acids 98 to 131 is required for ERK5 binding. The results also demonstrate that the previously proposed MEK5 "docking site" for ERK5 encoded by amino acids 145 to 156 (26) is not essential for binding ERK5.

charged amino acids within residues 69 to 86. (C) ERK5 and MEKK2 pull-down assay using MEK5 sequences that encode the indicated amino acid sequences (18 to 165, etc.). The assay was conducted as in panel A. A nonspecific band in the anti-HA blot is marked with an asterisk. (D) Binding in cells of ERK5 with MEK5 sequences that encode the indicated amino acid sequences. The assay was conducted as in panel B. The anomalous reversion of mobility of the 36-144 and 48-144 deletion proteins is presumably produced by the loss of negatively charged amino acids within residues 36 to 47. (E) Mapping of residues required for the MEK5 PB1 domain binding of ERK5. The analysis was carried out as in panel A.

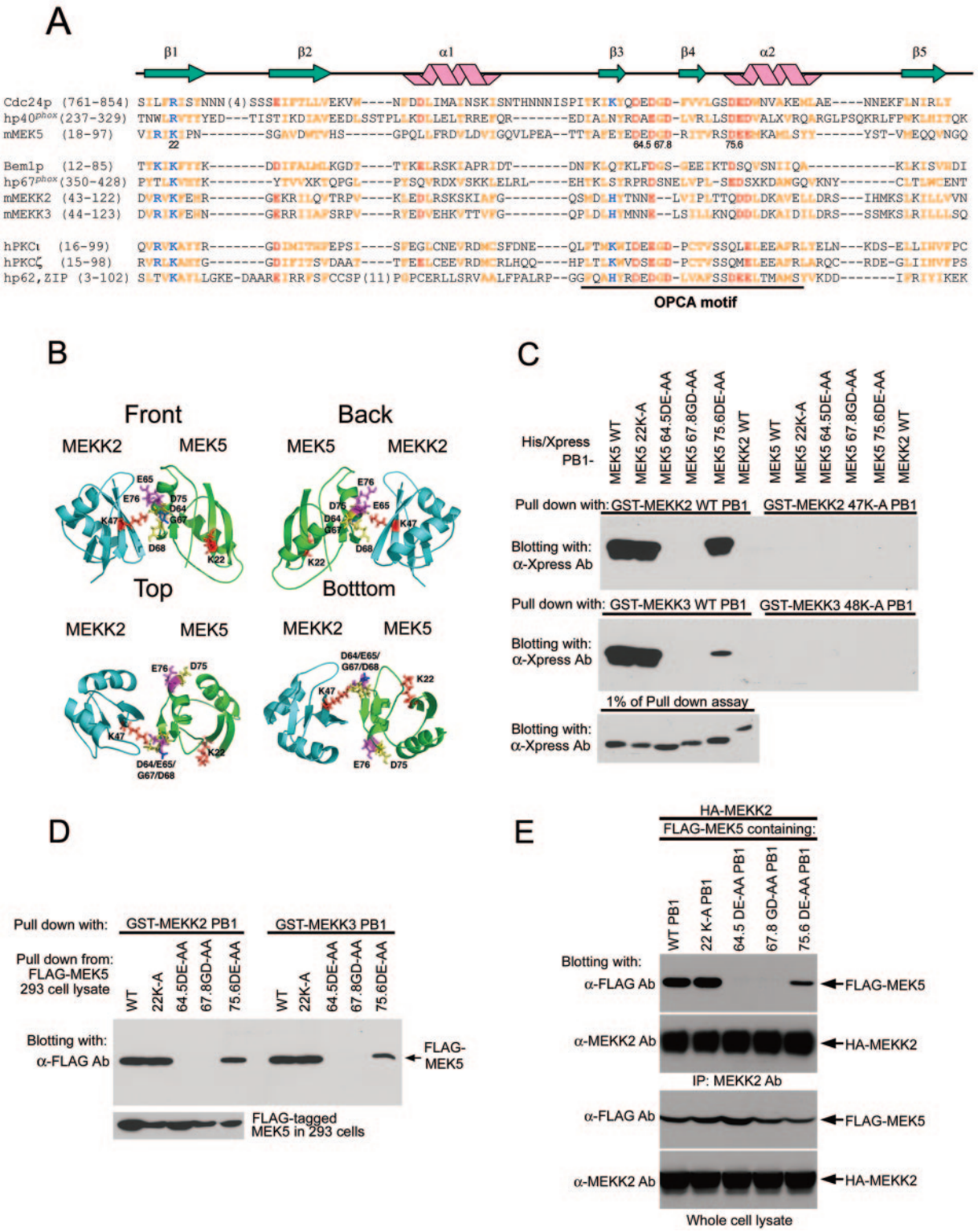

FIG. 3. Amino acid interactions involved in the heterodimerization of MEK5 and MEKK2 PB1 domains. (A) Sequence alignment of PB1 domains from different proteins. Secondary structure predictions are based on the reported structures of the Cdc24p and Bem1p PB1 domains (27). Conserved basic, acidic, and hydrophobic residues are shown in blue, red, and yellow, respectively. (B) Three-dimensional homology models of MEKK2 and MEK5 PB1 domains predict an interaction mediated by basic and acidic residues. Homology models of MEKK2 (cyan ribbon structures) and MEK5 (green ribbon structures) PB1 domains were oriented in the same positions as the bipartite crystal structure of the $p67^{phox}/p40^{phox}$ complex (31). The interface of MEKK2 and MEK5 is predicted to involve the interaction of lysine 47 (^{47}K) of MEKK2 with the first acidic cluster (AC1) of the MEK5 PB1 domain. Residues mutated in MEKK2 and MEK5 are indicated (D, yellow; E, magenta; G, blue; K, red). (C) Pull-down assays were conducted with GST fusion proteins of the PB1 domains of WT or ^{47}K-A MEKK2, WT or ^{48}K-A MEKK3, and His/Xpress-tagged WT or mutant MEK5 PB1 domains. (The nomenclature in the figure represents ^{64}D^{65}E-AA as $^{64.5}$DE-AA, etc.) The WT

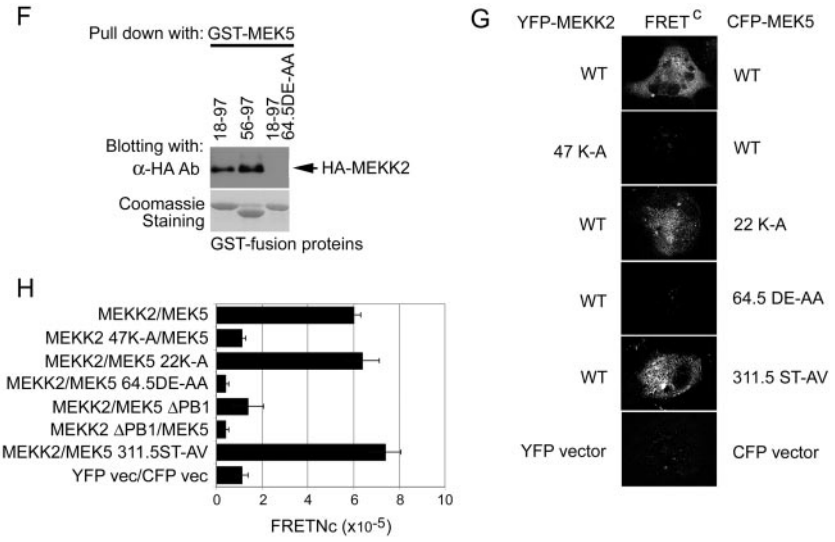

FIG. 3—*Continued.*

Stimulus-induced FRET^c changes measure the regulation of MEKK2-MEK5 and MEK5-ERK5 interactions and activation. FRET has the ability to detect protein interactions in living cells, and we used live cell FRET^c measurements to measure the interaction of YFP-MEKK2 with CFP-MEK5 and of CFP-MEK5 with YFP-ERK5 in response to stimulation of the ERK5 pathway. We observed a significant basal FRET^c with YFP-MEKK2/CFP-MEK5 interaction (Fig. 3G and H and 5A and C), indicating that MEKK2 and MEK5 are in a complex in resting cells. Sorbitol is a strong activator of the ERK5 pathway (13, 17), and sorbitol stimulation enhanced the FRET^c/CFP ratio ~2.4-fold, which represents a statistically significant change in the interaction of YFP-MEKK2 and CFP-MEK5 (Fig. 5A and C). The FRET^c increase is associated with activation of the pathway. The maximum FRET^c change was detected at 1 min after sorbitol challenge, the earliest time we can measure, with the FRET^c value gradually decreasing over time. The YFP and CFP fluorescence shown in Fig. 5A (left two panels) indicate that the time-dependent decrease in FRET^c is not simply due to bleaching of the dyes. MEKK2 phosphorylation is correlated with an upward mobility shift associated with its activation which increases over the time of stimulus-induced FRET^c changes (Fig. 5C). Coexpression of ERK5 with YFP-MEKK2 and CFP-MEK5 did not alter FRET^c (Fig. 5A), consistent with the mutation analysis that showed ERK5 does not compete with MEKK2 for binding to MEK5. In addition, expression of a constitutively active CFP-MEK5 (^{311}S^{315}T-DD CFP-MEK5) did not alter FRET^c measured for the interaction of CFP-MEK5 with YFP-MEKK2 (Fig. 5A). The findings indicate that MEKK2 and MEK5 can exist in a complex independent of the activation state of MEK5.

The ^{47}K-A mutation in the PB1 domain of MEKK2 causes a complete loss of MEKK2-MEK5 interaction with essentially complete loss of basal FRET^c and no significant sorbitol-induced FRET^c change when YFP-^{47}K-A MEKK2 is coexpressed with CFP-MEK5 (Fig. 5A and D). The mutation of

MEKK2 PB1 domain was used to show it did not dimerize with itself or the MEKK3 PB1 domain. The GST fusion protein adsorbents were resolved and immunoblotted with anti-Xpress antibody (for MEK5 PB1 domains). The bottom panel shows the anti-Xpress immunoblot of 1% of total His/Xpress-tagged proteins used for the pull-down assays. (D) Full-length FLAG-tagged WT or PB1 domain mutant MEK5 proteins were used in pull-down assays with GST-MEKK2 or GST-MEKK3 PB1 domains and immunoblotted with anti-FLAG antibody. The bottom panel shows an anti-FLAG blot of transfected HEK293 cell lysates (100 μg, with 10% of input 293 lysate for each pull-down assay) demonstrating equivalent expression of FLAG-tagged MEK5 for each construct. (The nomenclature in the figure represents ^{64}D^{65}E-AA as $^{64.5}$DE-AA, etc.) (E) Full-length FLAG-tagged WT and PB1 domain mutated MEK5 and MEKK2 proteins were transiently expressed in HEK293 cells. HA-MEKK2 protein was immunoprecipitated from the cells by using an anti-MEKK2 monoclonal antibody. The immunocomplexes were analyzed by anti-FLAG immunoblotting. The bottom panel shows the expression of FLAG-tagged MEK5 and HA-MEKK2. (The nomenclature in the figure represents ^{64}D^{65}E-AA as $^{64.5}$DE-AA, etc.) (F) HA-MEKK2 pull-down assay using a GST fusion protein encoding the MEK5 C-terminal PB1 domain moiety. GST-MEK5 fusions encoding the entire PB1 domain (amino acids 18 to 97), C-terminal PB1 moiety (amino acids 56 to 97), or ^{64}D^{65}E-AA PB1 in the full-length PB1 domain (amino acids 18 to 97) were tested for binding of MEKK2. The absorbents were resolved and blotted with anti-HA antibody. The amount of GST fusion protein used in each assay is shown by Coomassie blue staining (bottom panel). (G) In vivo interaction of MEK5 and MEKK2 detected using micro-FRET analysis. MEK5 (WT, ^{22}K-A, ^{64}D^{65}E-AA, and ^{311}S^{315}T-AV) in pECFP-C and MEKK2 (WT and ^{47}K-A) in pEYFP-C were coexpressed in COS7 cells. CFP, YFP, and FRET channel signals in live cells were captured by using a three-filter FRET microscope setup. Corrected FRET (FRET^c) images were created by using micro-FRET subtraction methods. The fluorescence signal was evaluated in the same dynamic range throughout the FRET^c image analysis. A control FRET^c between empty YFP-C and CFP-C vectors is shown in the bottom panel. (H) Data analysis of micro-FRET data using WT, ^{22}K-A, ^{64}D^{65}E-AA, or ^{311}S^{315}T-AV full-length or PB1 domain-deleted (ΔPB1) MEK5 and WT or ^{47}K-A full-length or ΔPB1 MEKK2. The data are represented as the mean FRETN^c value ± the standard deviation (SD) for multiple images (n = 5 to 8). FRETN^c between empty YFP and CFP vectors is also shown as a control.

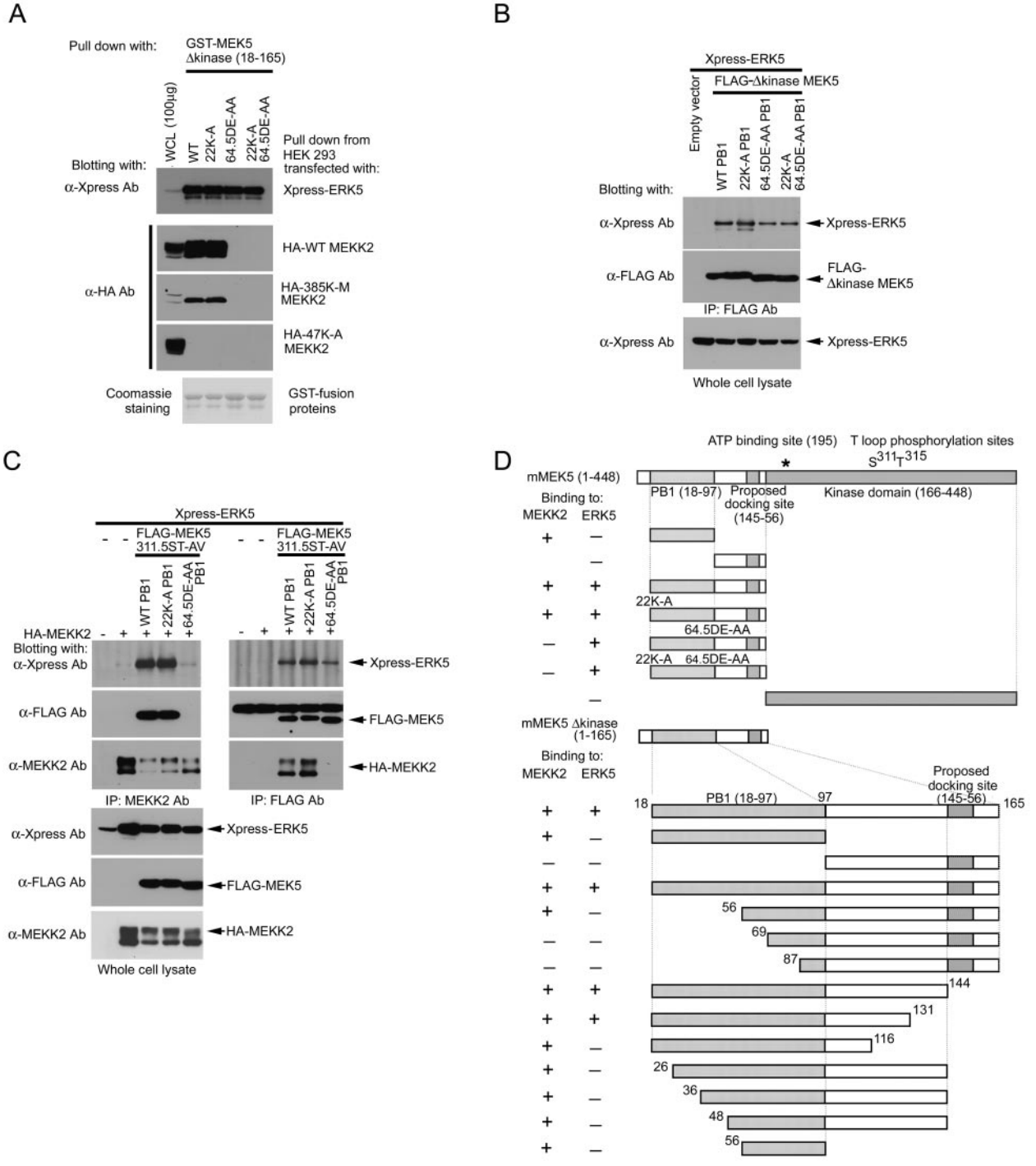

FIG. 4. Mapping of MEK5 PB1 domain amino acids required for ERK5 and MEKK2 binding. (A) ERK5 and MEKK2 binding to MEK5 were analyzed by using GST-Δkinase MEK5(18-165) with the indicated mutations in the MEK5 PB1 domain, ERK5, and MEKK2 WT or mutant of active-site lysine or conserved PB1 domain lysine. MEK5 GST fusions were used to test for binding to Xpress-ERK5 and HA-MEKK2 (WT, ^{47}K-A, and ^{385}K-M). The adsorbents along with 100 μg (10% of the lysates used for pull-down assay) of each whole-cell lysate were analyzed with anti-Xpress or anti-HA blotting. A nonspecific band in the anti-HA blot is marked with an asterisk. The bottom panel shows the GST fusion proteins used in the assay. (Nomenclature in the figures represents ^{64}D^{65}E-AA as $^{64.5}$DE-AA, etc.) (B) Binding of ERK5 and Δkinase MEK5 mutants in cells. Xpress-ERK5 and FLAG-Δkinase MEK5(1-165) mutant proteins were coexpressed in HEK293 cells. Anti-FLAG antibody immunoprecipitates were analyzed with anti-Xpress antibody for ERK5. The bottom panel shows the equivalent expression of Xpress-ERK5 in each transfectant. (C) FLAG-tagged PB1 domain mutants of ^{311}S^{315}T-AV MEK5 and Xpress-tagged ERK5 with or without HA-tagged MEKK2 were expressed in HEK293 cells. HA-MEKK2 and FLAG-MEK5 were immunoprecipitated with anti-MEKK2 (top left panel) and anti-FLAG (top right panel) antibodies, respectively. The immunocomplexes were analyzed with anti-Xpress (for ERK5), anti-FLAG (for MEK5), and anti-MEKK2 antibodies. The bottom panel shows the expression of ERK5, MEK5, and MEKK2 proteins. (D) Map of ERK5 and MEKK2 binding sites in MEK5. The map was created based on assays shown in Fig. 1 to 4 and on additional deletion and mutation analysis experiments.

^{311}S and ^{315}T in the T loop of MEK5 (^{311}S^{315}T-AV MEK5) inhibits MEK5 phosphorylation and activation by MEKK2. FRET^c values are similar with WT MEK5 or ^{311}S^{315}T-AV MEK5 and WT MEKK2, indicating both MEK5 proteins are in a complex with MEKK2 in resting cells (Fig. 5A and E). However, the sorbitol-induced FRET^c increase observed with WT MEKK2 and MEK5 is lost with ^{311}S^{315}T-AV MEK5, and the basal FRET^c simply trends downward after sorbitol stimulation. Thus, MEKK2 catalyzed MEK5 phosphorylation contributes to the sorbitol-induced change in MEKK2-MEK5 interaction and the increase in observed FRET^c in the PB1 domain organized signaling complex.

In contrast to the behavior of YFP-MEKK2 and CFP-MEK5, CFP-MEK5 and YFP-ERK5 have a very low basal FRET^c in resting cells (Fig. 5B and F). The lack of FRET must be related to the orientation of the CFP and YFP, since the MEK5 and ERK5 proteins can be coimmunoprecipitated in a complex in resting cells. Upon sorbitol stimulation there is a significant sixfold increase in CFP-MEK5/YFP-ERK5-induced FRET^c. The increase in FRET^c after sorbitol treatment is followed by the accumulation of phosphorylated ERK5 (Fig. 5F, immunoblots). Deletion of the MEK5 PB1 domain (ΔPB1) causes essentially a complete loss of MEK5-ERK5 FRET^c and ERK5 phosphorylation (Fig. 5B and G). This finding in living cells substantiates the absolute requirement of the MEK5 PB1 domain for MEK5-ERK5 interaction. Furthermore, mutation of the MEK5 T loop phosphorylation sites (^{311}S^{315}T-AV MEK5), which blocks MEK5 activation, inhibits the sorbitol-induced FRET^c increase seen with CFP-WT MEK5 and YFP-ERK5 and ERK5 phosphorylation (Fig. 5B and H). Thus, activation of MEK5 is required for the sorbitol-induced increase in FRET^c associated with MEK5 and ERK5 activation. As observed with MEKK2 and MEK5 interaction, there is a time-dependent decay in MEK5-ERK5 FRET^c. The YFP and CFP channels in Fig. 5B (left two panels) show that the decay in FRET^c is not due to significant photobleaching of the dyes. The decay in FRET^c observed with sorbitol stimulation is therefore due to conformational changes and/or dissociation of proteins in the complex. Coexpression of MEKK2 with YFP-ERK5 and CFP-MEK5 caused a loss of FRET^c (Fig. 5B). A significant fraction of MEKK2 when expressed by transfection is in an activated state, as shown by the higher gel band in the MEKK2 blots (Fig. 5C, D, and E). Thus, MEK5 and ERK5 become activated when MEKK2 is overexpressed in cells and, by 24 to 48 h posttransfection, most of the YFP-ERK5 is in the nucleus (not shown). Expression of YFP-ERK5 with constitutively active CFP-MEK5 (^{311}S^{315}T-DD MEK5) also results in a loss of FRET^c (Fig. 5B), with much of the ERK5 in the nucleus, similar to what is seen with overexpression of MEKK2 (not shown). Combined, these findings in living cells indicate that upon sorbitol stimulation there is an initial increase in FRET^c related to apparent conformational changes in the interaction of CFP-MEK5 and YFP-ERK5 and the loss of FRET^c correlates with conformational changes and dissociation of the two proteins.

MEKK2-MEK5-ERK5 ternary complex is required for ERK5 activation. Figure 6 shows that the MEKK2 PB1 domain is capable of forming a ternary complex in vitro with MEK5 and ERK5 (panel A), a finding consistent with MEKK2 and ERK5 having noncompeting binding sites associated with the MEK5 PB1 domain (see also Fig. 1C and 6C). The in vitro formation MEK5 complexes with MEKK2 and ERK5 are independent of the order of addition of MEKK2 and ERK5 (Fig. 6B), and the MEK5 PB1 domain-dependent complexes are required for MEKK2 activation of ERK5 (Fig. 6C and D). Inhibition of MEKK2-MEK5 interaction by mutation of the acidic cluster of the MEK5 PB1 domain or deletion of the ERK5 binding sites within residues 18 to 25 or residues 117 to 131 in MEK5 causes a loss of ERK5 phosphorylation associated with ERK5 activation. FRET^c analysis in the absence and presence of sorbitol confirms deletion of MEK5 residues 117 to 131 results in loss of MEK5-ERK5 interaction but not MEKK2-MEK5 interaction (Fig. 6E), and deletion of this sequence inhibits the ability of a constitutively active MEK5, with aspartate residues replacing ^{311}S^{315}T (^{311}S^{315}T-DD MEK5) in the MEK5 activation loop, to activate ERK5 (Fig. 6F). ERK5 activation, coimmunoprecipitation of PB1 domain-dependent complexes and FRET^c analysis cumulatively demonstrate that residues 18 to 25 in the PB1 domain and residues 117 to 131 in the C-terminal extension are both essential for MEK5 binding and activation of ERK5.

MEK5 PB1 domain confers ERK5 binding and activation by a PB1-MEK1 fusion protein. To unequivocally prove the requirement of the MEK5 PB1 domain in regulating ERK5, it was fused in frame with MEK1, the MAP2K that regulates ERK1 and -2. Constitutively active MEK1 with serines 218 and 222 in the T loop mutated to glutamate and aspartate (^{218}S^{222}S-ED MEK1), respectively, was used in the analysis. Figure 7 shows that a MEK5 PB1 domain-MEK1 fusion binds ERK5 (left panel). Deletion of the N-terminal moiety of the MEK5 PB1 domain (Δ18-25) or the C-terminal extension (Δ117-131) resulted in loss of ERK5 binding to the PB1-MEK1 chimera. The WT PB1 domain fused to MEK1 is capable of phosphorylating ERK5, but the Δ18-25 and Δ117-131 PB1-MEK1 proteins do not phosphorylate ERK5 (Fig. 7, right panel). Binding and phosphorylation of ERK5 by the activated MEK5 PB1 domain-MEK1 fusion protein is independent of MEKK2 binding, as shown with the MEK5 ^{64}D^{65}E-AA PB1 domain mutant that no longer binds MEKK2. In contrast, the WT and mutant PB1-MEK1 proteins all phosphorylate ERK1/2. The findings clearly demonstrate that the MEK5 PB1 domain and the 34-amino-acid C-terminal extension bind ERK5, and placement of this sequence at the N terminus of an unrelated MAP2K, MEK1, confers a PB1 domain-dependent regulation of ERK5 in addition to the normal MEK1 function of phosphorylating and activating ERK1/2.

DISCUSSION

We define here the function of the MEK5 PB1 domain as a scaffold for the formation of a ternary signaling complex required for ERK5 activation. This is a unique function for a PB1 domain in forming a MEKK2 (or MEKK3)-MEK5-ERK5 ternary complex. No other MAPK cascade has been shown to form such a complex. Only the C-terminal moiety of the MEK5 PB1 domain is required for MEKK2 (or MEKK3) binding. Mapping of the ERK5-binding domain demonstrated that residues from 18 to 25 in the N-terminal moiety of the PB1 domain and residues 117 to 131 C terminal to the PB1 domain are required for ERK5 binding. There is ample precedent for

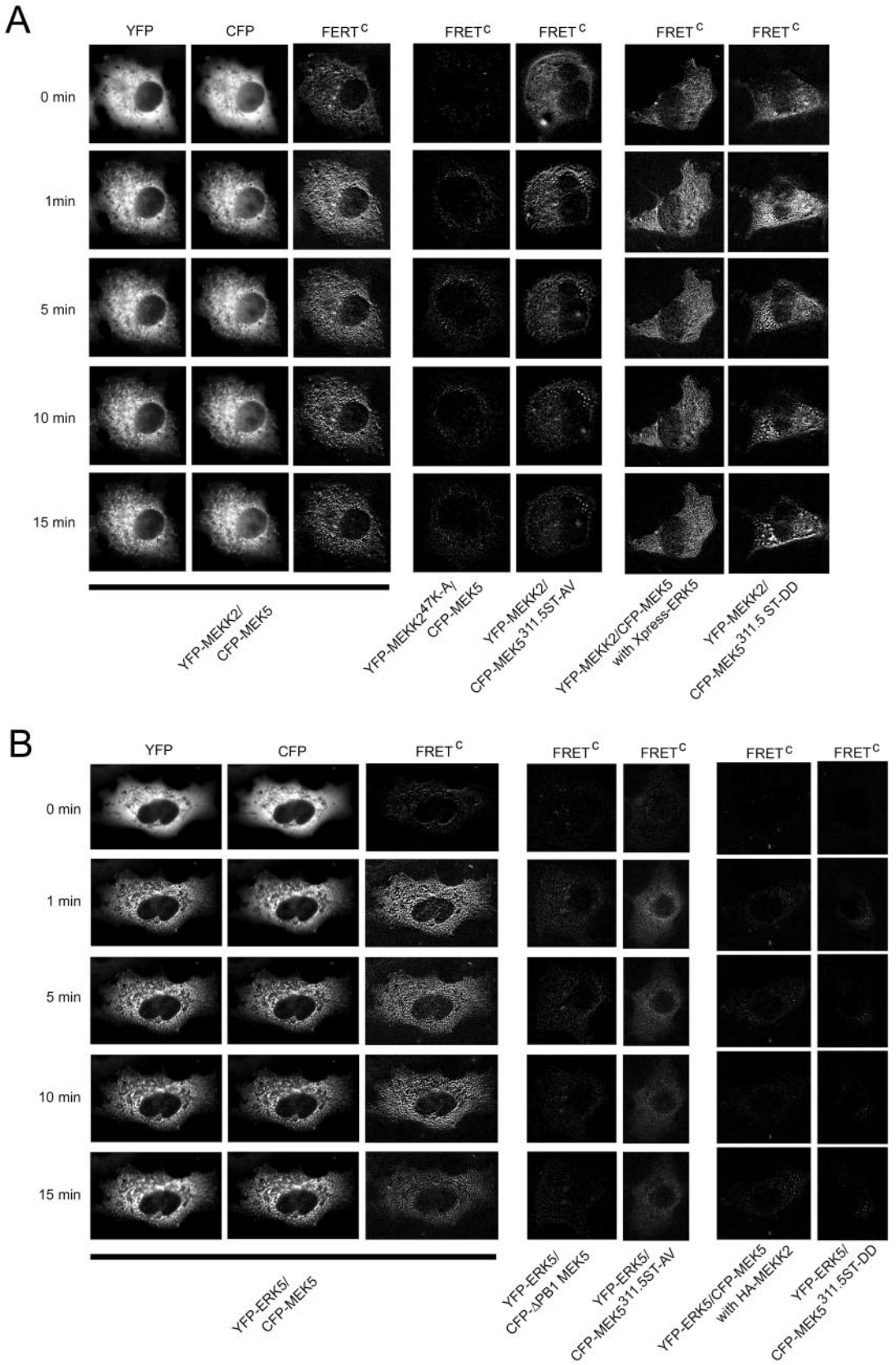

FIG. 5. Sorbitol-induced micro-FRET changes for MEKK2/MEK5 and MEK5/ERK5 interactions. (A) CFP-WT MEK5 and YFP-WT MEKK2 were coexpressed in COS7 cells. After 4 h of serum starvation, cells were stimulated with 200 mM sorbitol. Images were captured at the indicated time points after sorbitol stimulation. YFP, CFP, and FRET^c images are shown in the three left columns. The FRET^c signals

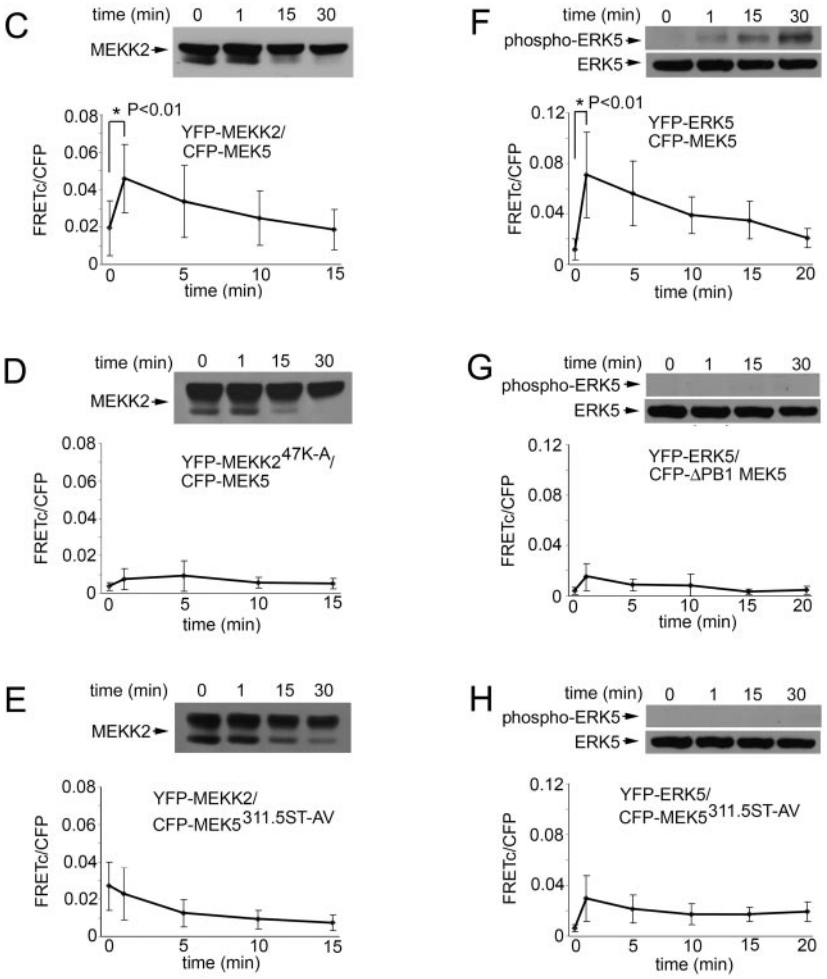

FIG. 5—*Continued.*

such extended roles of specific domains contributing to the function of a second interaction domain or motif. A good example is the pleckstrin homology domain of the β-adrenergic receptor kinase, whose extended C-terminal sequence is required for binding Gβγ (3), similar to the role of the extended C terminus of the MEK5 PB1 domain. Other domains also have been shown to use different surfaces to bind more than one ligand. For example, the Disabled-1 (Dab-1) phosphotyrosine binding (PTB) domain simultaneously binds both phosphoinositide and peptide ligands at different surfaces of

between CFP-MEK5 and YFP-^{47}K-A MEKK2 and between CFP-^{311}S^{315}T-AV MEK5 and YFP-MEKK2 are presented in the middle two columns. The FRET^c images between CFP-MEK5 and YFP-MEKK2 in the presence of Xpress-ERK5 and CFP-^{311}S^{315}T-DD MEK5 and YFP-MEKK2 are shown in the right two columns. (B) Time course of FRET^c between CFP-WT MEK5 and YFP-WT ERK5 in COS7 cells stimulated with 200 mM sorbitol (left three columns). The middle two columns represent FRET^c time courses for CFP-PB1 domain-deleted MEK5 (ΔPB1 MEK5) and YFP-ERK5 and for CFP-^{311}S^{315}T-AV MEK5 and YFP-ERK5. The FRET^c images between CFP-MEK5 and YFP-ERK5 in the presence of HA-MEKK2 and CFP-^{311}S^{315}T-DD MEK5 and YFP-ERK5 are shown in the right two columns. (C, D, and E) Analysis of the changes in FRET^c/CFP between CFP-MEK5 and YFP-MEKK2 after sorbitol stimulation. FRET^c/CFP between CFP-MEK5 and YFP-MEKK2 (C), CFP-MEK5 and YFP-^{47}K-A MEKK2 (D), and CFP-^{311}S^{315}T-AV MEK5 (designated $^{311.315}$ST-AV MEK5 in figure) and YFP-MEKK2 (E) was evaluated. The value of FRET^c divided by CFP (FRET^c/CFP) ± the SD for multiple images ($n = 5$ to 7) was used for statistical analysis of multiple experiments. The results shown are in each case representative of three replicate experiments. The asterisk in panel C indicates statistical significance ($P < 0.01$) between the cells at time zero and at 1 min as determined by paired *t* test. (C to E, inset) Anti-MEKK2 antibody blot of WT or ^{47}K-A MEKK2 expressed in COS7 cells harvested at the indicated times after sorbitol stimulation showing the MEKK2 gel shift that correlates with MEKK2 activation. (F to H) Data analyses of the FRET^c/CFP kinetics between CFP-MEK5 and YFP-ERK5 after sorbitol stimulation. FRET between CFP-MEK5 and YFP-ERK5 (F), CFP-ΔPB1 MEK5 and YFP-ERK5 (G), and CFP-^{311}S^{315}T-AV MEK5 and YFP-ERK5 (H) was calculated as FRET^c/CFP ± the SD for multiple images ($n = 6$). The results shown are in each case representative of three replicate experiments. The asterisk in panel F indicates statistical significance ($P < 0.01$) versus the cells at time zero as determined by paired *t* test. (F to H, inset) Anti-phospho-ERK5 and anti-ERK5 antibody blots at the indicated time point after sorbitol stimulation.

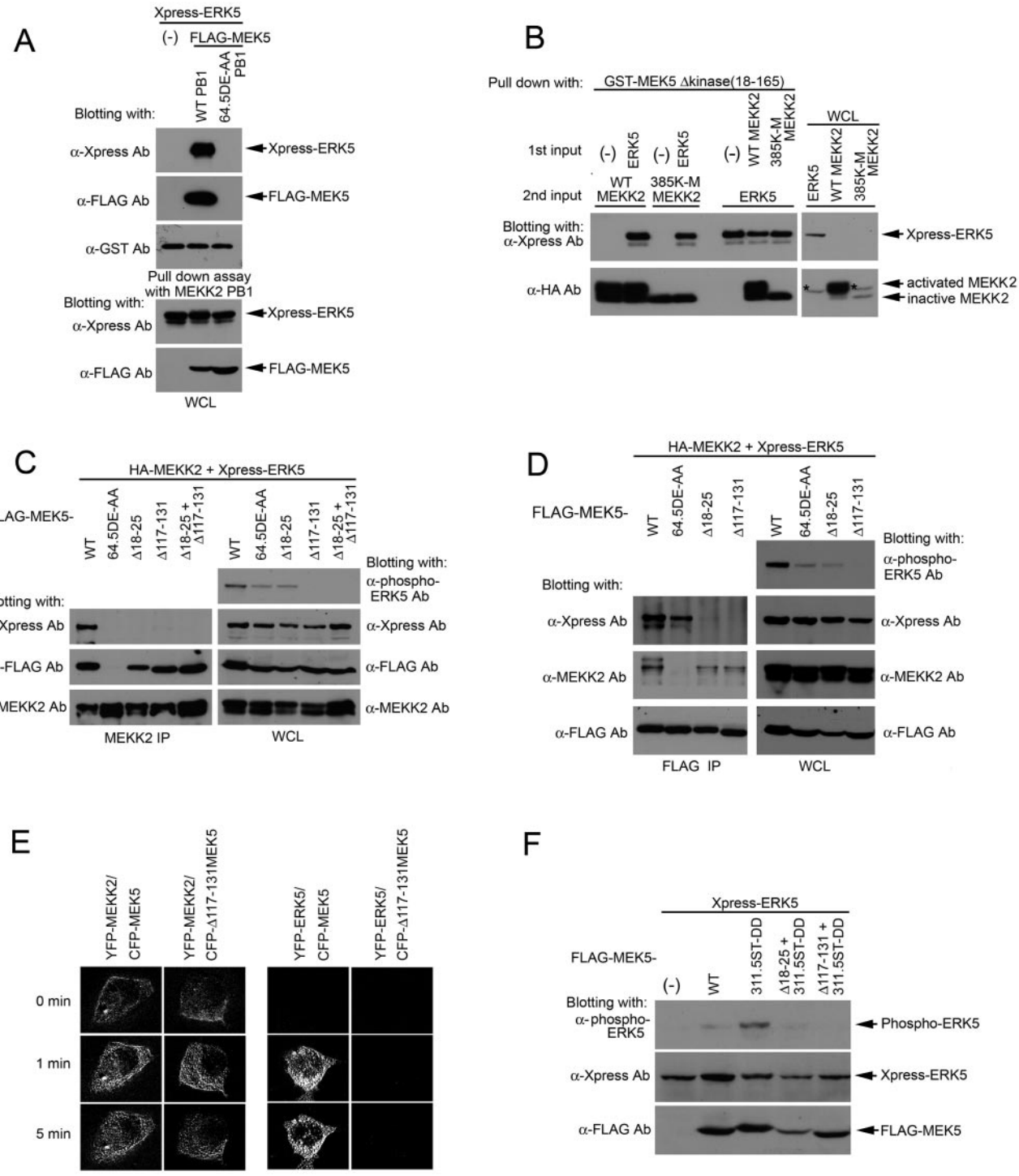

FIG. 6. Amino acid requirements for MEK5 PB1 domain formation of a ternary complex with MEKK2 and ERK5. (A) MEK5-ERK5 complexes isolated by MEKK2-MEK5 PB1 domain interactions. Xpress-ERK5 and FLAG-WT or PB1 mutated (^{64}D^{65}E-AA) full-length MEK5 were coexpressed in HEK293 cells. Pull-down assays were performed by using a GST-MEKK2 PB1 domain. ERK5 and MEK5 in the complex were detected with anti-Xpress and anti-FLAG antibodies, respectively. The equivalent expression of each protein was confirmed by whole-cell lysate blot (bottom panel). (The nomenclature in the figure represents ^{64}D^{65}E-AA as $^{64.5}$DE-AA, etc.) (B) In vitro reconstitution of a MEKK2-MEK5-ERK5 ternary complex. For the first input, GST-Δkinase MEK5(18-165) was used to bind either ERK5 or WT or ^{385}K-M MEKK2 proteins, and the beads were extensively washed with lysis buffer. For the second input, ERK5 bound beads were incubated with the MEKK2 and MEKK2-bound beads were incubated with ERK5, respectively. The absorbents were blotted with anti-Xpress (for ERK5) and anti-HA (for MEKK2) antibodies. Blots of whole-cell lysates confirmed the expression of each protein (right panel). A nonspecific band in the anti-HA blots is marked with an asterisk. (C) FLAG-tagged MEK5 proteins (WT, ^{64}D^{65}E-AA, Δ18-25, Δ117-131, Δ18-25, and Δ117-131), Xpress-tagged ERK5, and HA-tagged MEKK2 were expressed in HEK293 cells. HA-MEKK2 was immunoprecipitated from the cell lysates with anti-MEKK2 antibody. The HA-MEKK2 immunocomplexes (left panel) and whole-cell lysates (right panel) were analyzed with anti-Xpress (for ERK5), anti-FLAG

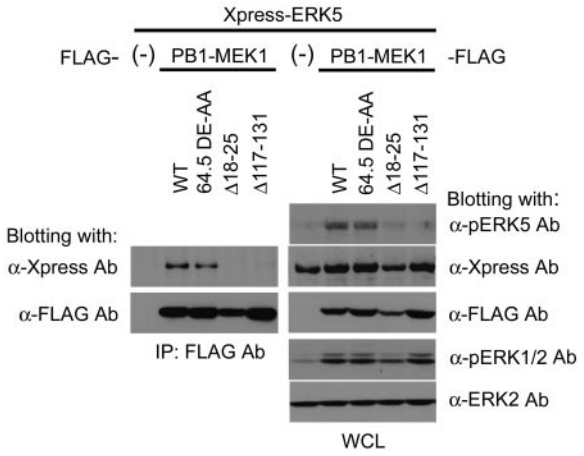

FIG. 7. The MEK5 PB1 domain fused to MEK1 confers specific ERK5 binding and activation. FLAG-MEK5 constructs encoding amino acids 1 to 131 (PB1 domain plus 34-residue C-terminal extension) with either the WT sequence or harboring the ^{64}D^{65}E-AA mutation or the 18-25 or 117-131 deletions were fused to the N terminus of constitutively activated MEK1. These constructs were coexpressed with X-press-ERK5, and complexes were immunoprecipitated with anti-FLAG antibody and blotted with anti-Xpress or anti-FLAG antibodies (left panel). The whole-cell lysate of each transfectant was subjected to sequential blotting with anti-phospho-ERK5 antibody for activation of ERK5, anti-Xpress antibody (for ERK5), anti-FLAG antibody (for MEK5), anti-phospho-ERK1/2 antibody for activation of ERK1/2, and ERK2 antibody (right panel).

the PTB domain (33). The Pex13p SH3 domain simultaneously binds the Pex5p and Pex14p proteins on opposite surfaces (7), and the SAP SH2 domain has been shown to bind the Fyn SH3 domain and the SLAM cytoplasmic tail on opposite surfaces (4).

FRET^c analysis clearly demonstrated that MEKK2 and MEK5 are in a stable complex in living cells that is dependent on PB1-PB1 domain interactions. Stimulation of the ERK5 pathway by exposure of cells to sorbitol induced a significant FRET^c change between YFP-MEKK2 and CFP-MEK5, which requires both MEKK2 activation and the subsequent phosphorylation of ^{311}S and ^{315}T in the T loop of MEK5. The decline in FRET^c observed with sorbitol stimulation also reflects changes in the dynamics of MEKK2 and MEK5 interaction. Both the increase and the decay of FRET^c in response to sorbitol must therefore result from changes in the interaction of YFP-MEKK2 and CFP-MEK5. Dissociation of the complex, stimulus-dependent conformational changes and proteins interacting with MEKK2, such as Mip1 (6), probably contribute to the observed FRET^c response to sorbitol.

CFP-MEK5 and YFP-ERK5 do not give a significant FRET^c signal in resting cells but rapidly induce a robust FRET^c in response to sorbitol. There are several potential reasons related to distance and orientation of CFP-MEK5 and YFP-ERK5 that they do not give FRET^c in a basal, unstimulated complex. The stimulus-induced MEK5-ERK5 FRET^c increase requires a functional MEK5-MEKK2 PB1 domain heterodimer, MEKK2-dependent phosphorylation of MEK5, and a kinase-active MEK5 for phosphorylation of ERK5. With overexpression of MEKK2 or a constitutively active MEK5, ERK5 appears to dissociate from the complex, and much of the ERK5 protein is translocated to the nucleus. The ability to visualize stimulus-induced FRET^c changes is the first demonstration of a FRET-based assay for the measurement of protein interactions and activation of a MAPK cascade. Our studies define the ability to essentially perform single living cell biochemistry to study the dynamic behaviors of a MAPK pathway.

It is important to note that our findings differ significantly from the recent report by Seyfried et al. (23). In that study the authors mapped residues ^{63}EDED^{66} within the OPCA motif of the MEK5 PB1 domain as important for binding to MEKK2 (or MEKK3) and ERK5. These authors proposed a model whereby MEKK2 or (MEKK3) is bound to MEK5 and, when the MAP3K activates MEK5, they dissociate, allowing ERK5 binding to the same site and subsequent ERK5 activation. Our findings are consistent with this sequence being critical for MEKK2 or MEKK3 binding to MEK5 but do not agree with this site being important for ERK5 binding. A possible explanation is the mutations that were made in the study by Seyfried et al. These authors mutated the acidic cluster ^{63}EDED^{66} to the bulky hydrophobic sequence LVLV, whereas we mutated the acidic cluster residues to alanines. Our characterization of the MEK5 PB1 domain suggests the introduction of such hydrophobic residues might disrupt the structure of the PB1 domain that would consequently cause loss of binding to both MEKK2 or MEKK3 and ERK5. In our studies we were careful to show that mutations that inhibit MEKK2 or MEKK3 binding do not affect ERK5 binding and vice versa.

Recently, Takekawa et al. (25) defined a DVD (domain for versatile docking) site in MEK1, MKK4/7, and MKK3/6 that binds specific MAP3Ks such as Raf1, ASK1, TAK1, MEKK1, and MEKK4 (MTK1). The DVD site resides just C terminal of the kinase domain of these MAP2Ks. The MAP2K DVD site was shown to be required for MAP3K activation of the

(for MEK5), and anti-MEKK2 antibodies. In addition, whole-cell lysates were blotted with anti-phospho-ERK5 antibody that measures activated ERK5. (D) FLAG-tagged MEK5 WT and mutant proteins were expressed with Xpress-ERK5 and HA-MEKK2. Complexes were immunoprecipitated with anti-FLAG antibody. Immunoprecipitates (left panel) and whole-cell lysates (right panel) were sequentially analyzed with anti-Xpress (ERK5), anti-FLAG (MEK5), and anti-MEKK2 antibodies. Whole-cell lysates were also blotted with anti-phopho-ERK5 antibody for the measurement of ERK5 activation. (E) FRET analysis of MEK5-ERK5 interaction in living cells. WT- and Δ117-131 MEK5-CFP fusion proteins were coexpressed with YFP-WT MEKK2 (left panel) or YFP-ERK5 proteins in COS7 cells (right panel). After 4 h of serum starvation, the cells were stimulated with 200 mM sorbitol. The images were captured at the indicated time points and processed to obtain FRET^c images. The images shown are representative of FRET^c kinetics from three to five cells in two independent experiments with the FRET^c images presented in the same dynamic range. (F) FLAG-WT MEK5 or constitutively active ^{311}S^{315}T-DD MEK5 or two different truncation proteins with deletions of amino acids 18 to 25 or amino acids 117 to 131 in the background of ^{311}S^{315}T-DD mutant MEK5 were coexpressed with Xpress-ERK5. Whole-cell lysates of each condition were blotted sequentially with antibodies for phospho-ERK5 to measure ERK5 activation, Xpress to measure ERK5 protein, and FLAG to measure MEK5 protein.

MAP2K. Interestingly, MEK5 also has a DVD site C terminal to the kinase domain encoded by the sequence ^{416}HPFIVQ FNDGNSTVVSMWVCRALE^{439}. The N lobe surrounding the active-site lysine of the MAP3K kinase domain was shown to bind to such a DVD site in other MAP2Ks. We have found that MEKK2 binds MEK1 independent of the MEKK2 PB1 domain, presumably via a MEK1 DVD-MEKK2 N lobe interaction (unpublished observation). The findings indicate that MEKK2 can bind specific MAP2Ks such as MEK1 independent of the PB1 domain but that the MEKK2-MEK5 interaction has an absolute requirement for PB1 domain heterodimerization.

The ternary complex of MEKK2 (or MEKK3), MEK5, and ERK5 organized by the MEK5 PB1 domain is unique among MAP2Ks and independent of the DVD site. As the name "domain for versatile docking" implies, specific MAP2Ks interact with multiple MAP3Ks. In fact, there are more than 20 defined MAP3Ks and only 7 MAP2Ks for the regulation of ERK1/2, p38, JNK, and ERK5 (28). Thus, DVD sites are somewhat promiscuous, allowing different MAP3Ks to integrate upstream stimuli with the activation of multiple MAPKs. In contrast, only MEKK2, MEKK3, and MEK5 encode PB1 domains among all of the MAP3Ks and MAP2Ks, providing stringent specificity in their heterodimerization. Furthermore, the MEK5 PB1 domain docks ERK5; the ternary complex formed by the PB1 domain therefore confers a very stringent control of ERK5 activation by the two MAP3Ks with PB1 domains.

Some insight into the function of ERK5 was recently demonstrated by its targeted deletion in embryos and conditional deletion in adult mice. In mouse embryos ERK5 gene deletion was found to impair vascular development (22, 24, 32). In adult mice ERK5 was shown to be required for vascular integrity and endothelial cell survival (8). Deletion of ERK5 in the adult animal induced endothelial cell apoptosis and collapse of the vasculature. Thus, ERK5 is a critical MAPK for both development of the vasculature and vascular homeostasis in the adult, while no other MAPK has been shown to be critical in vascular maintenance in the adult animal. The MEK5 PB1 domain provides a unique and stringent PB1 domain heterodimerization mechanism for ERK5 activation by MEKK2 (or MEKK3) that is not used for the regulation of other MAPKs. Our findings implicate PB1 domain interactions in the ERK5 signaling complex as a novel therapeutic target to modulate vascularization in different human diseases.

ACKNOWLEDGMENTS

This study was supported NIH grants GM30324 and GM68820.

REFERENCES

1. **Akaike, M., W. Che, N. L. Marmarosh, S. Ohta, M. Osawa, B. Ding, B. C. Berk, C. Yan, and J. Abe.** 2004. The hinge-helix 1 region of peroxisome proliferator-activated receptor γ1 (PPARγ1) mediates interaction with extracellular signal-regulated kinase 5 and PPARγ1 transcriptional activation: involvement in flow-induced PPARγ activation in endothelial cells. Mol. Cell. Biol. **24:**8691–8704.
2. **Cameron, S. J., S. Malik, M. Akaike, N. Lerner-Marmarosh, C. Yan, J. D. Lee, J. Abe, and J. Yang.** 2003. Regulation of epidermal growth factor-induced connexin 43 gap junction communication by big mitogen-activated protein kinase1/ERK5 but not ERK1/2 kinase activation. J. Biol. Chem. **278:**18682–18688.
3. **Carman, C. V., L. S. Barak, C. Chen, L. Y. Liu-Chen, J. J. Onorato, S. P. Kennedy, M. G. Caron, and J. L. Benovic.** 2000. Mutational analysis of Gβγ and phospholipid interaction with G protein-coupled receptor kinase 2. J. Biol. Chem. **275:**10443–10452.
4. **Chan, B., A. Lanyi, H. K. Song, J. Griesbach, M. Simarro-Grande, F. Poy, D. Howie, J. Sumegi, C. Terhorst, and M. J. Eck.** 2003. SAP couples Fyn to SLAM immune receptors. Nat. Cell Biol. **5:**155–160.
5. **Chao, T. H., M. Hayashi, R. I. Tapping, Y. Kato, and J. D. Lee.** 1999. MEKK3 directly regulates MEK5 activity as part of the big mitogen-activated protein kinase 1 (BMK1) signaling pathway. J. Biol. Chem. **274:**36035–36038.
6. **Cheng, J., D. Zhang, K. Kim, Y. Zhao, and B. Su.** 2005. Mip1, an MEKK2-interacting protein, controls MEKK2 dimerization and activation. Mol. Cell. Biol. **25:**5955–5964.
7. **Douangamath, A., F. V. Filipp, A. T. Klein, P. Barnett, P. Zou, T. Voorn-Brouwer, M. C. Vega, O. M. Mayans, M. Sattler, B. Distel, and M. Wilmanns.** 2002. Topography for independent binding of alpha-helical and PPII-helical ligands to a peroxisomal SH3 domain. Mol. Cell **10:**1007–1017.
8. **Hayashi, M., S. W. Kim, K. Imanaka-Yoshida, T. Yoshida, E. D. Abel, B. Eliceiri, Y. Yang, R. J. Ulevitch, and J. D. Lee.** 2004. Targeted deletion of BMK1/ERK5 in adult mice perturbs vascular integrity and leads to endothelial failure. J. Clin. Investig. **113:**1138–1148.
9. **Hayashi, M., and J. D. Lee.** 2004. Role of the BMK1/ERK5 signaling pathway: lessons from knockout mice. J. Mol. Med. **82:**800–808.
10. **Hayashi, M., R. I. Tapping, T. H. Chao, J. F. Lo, C. C. King, Y. Yang, and J. D. Lee.** 2001. BMK1 mediates growth factor-induced cell proliferation through direct cellular activation of serum and glucocorticoid-inducible kinase. J. Biol. Chem. **276:**8631–8634.
11. **Hirano, Y., S. Yoshinaga, K. Ogura, M. Yokochi, Y. Noda, H. Sumimoto, and F. Inagaki.** 2004. Solution structure of atypical protein kinase C PB1 domain and its mode of interaction with ZIP/p62 and MEK5. J. Biol. Chem. **279:**31883–31890.
12. **Kamakura, S., T. Moriguchi, and E. Nishida.** 1999. Activation of the protein kinase ERK5/BMK1 by receptor tyrosine kinases: identification and characterization of a signaling pathway to the nucleus. J. Biol. Chem. **274:**26563–26571.
13. **Kato, Y., V. V. Kravchenko, R. I. Tapping, J. Han, R. J. Ulevitch, and J. D. Lee.** 1997. BMK1/ERK5 regulates serum-induced early gene expression through transcription factor MEF2C. EMBO J. **16:**7054–7066.
14. **Kesavan, K., K. Lobel-Rice, W. Sun, R. Lapadat, S. Webb, G. L. Johnson, and T. P. Garrington.** 2004. MEKK2 regulates the coordinate activation of ERK5 and JNK in response to FGF-2 in fibroblasts. J. Cell Physiol. **199:**140–148.
15. **Lamark, T., M. Perander, H. Outzen, K. Kristiansen, A. Overvatn, E. Michaelsen, G. Bjorkoy, and T. Johansen.** 2003. Interaction codes within the family of mammalian Phox and Bem1p domain-containing proteins. J. Biol. Chem. **278:**34568–34581.
16. **Lee, J. D., R. J. Ulevitch, and J. Han.** 1995. Primary structure of BMK1: a new mammalian map kinase. Biochem. Biophys. Res. Commun. **213:**715–724.
17. **Nakamura, K., and G. L. Johnson.** 2003. PB1 domains of MEKK2 and MEKK3 interact with the MEK5 PB1 domain for activation of the ERK5 pathway. J. Biol. Chem. **278:**36989–36992.
18. **Nicol, R. L., N. Frey, G. Pearson, M. Cobb, J. Richardson, and E. N. Olson.** 2001. Activated MEK5 induces serial assembly of sarcomeres and eccentric cardiac hypertrophy. EMBO J. **20:**2757–2767.
19. **Oliveria, S. F., L. L. Gomez, and M. L. Dell'Acqua.** 2003. Imaging kinase–AKAP79–phosphatase scaffold complexes at the plasma membrane in living cells using FRET microscopy. J. Cell Biol. **160:**101–112.
20. **Pearson, G., J. M. English, M. A. White, and M. H. Cobb.** 2001. ERK5 and ERK2 cooperate to regulate NF-κB and cell transformation. J. Biol. Chem. **276:**7927–7931.
21. **Ponting, C. P., T. Ito, J. Moscat, M. T. Diaz-Meco, F. Inagaki, and H. Sumimoto.** 2002. OPR, PC and AID: all in the PB1 family. Trends Biochem. Sci. **27:**10.
22. **Regan, C. P., W. Li, D. M. Boucher, S. Spatz, M. S. Su, and K. Kuida.** 2002. Erk5 null mice display multiple extraembryonic vascular and embryonic cardiovascular defects. Proc. Natl. Acad. Sci. USA **99:**9248–9253.
23. **Seyfried, J., X. Wang, G. Kharebava, and C. Tournier.** 2005. A novel mitogen-activated protein kinase docking site in the N terminus of MEK5α organizes the components of the extracellular signal-regulated kinase 5 signaling pathway. Mol. Cell. Biol. **25:**9820–9828.
24. **Sohn, S. J., B. K. Sarvis, D. Cado, and A. Winoto.** 2002. ERK5 MAPK regulates embryonic angiogenesis and acts as a hypoxia-sensitive repressor of vascular endothelial growth factor expression. J. Biol. Chem. **277:**43344–43351.
25. **Takekawa, M., K. Tatebayashi, and H. Saito.** 2005. Conserved docking site is essential for activation of mammalian MAP kinase kinases by specific MAP kinase kinase kinases. Mol. Cell **18:**295–306.
26. **Tanoue, T., M. Adachi, T. Moriguchi, and E. Nishida.** 2000. A conserved docking motif in MAP kinases common to substrates, activators, and regulators. Nat. Cell Biol. **2:**110–116.
27. **Terasawa, H., Y. Noda, T. Ito, H. Hatanaka, S. Ichikawa, K. Ogura, H. Sumimoto, and F. Inagaki.** 2001. Structure and ligand recognition of the PB1

domain: a novel protein module binding to the PC motif. EMBO J. **20:**3947–3956.
28. **Uhlik, M. T., A. N. Abell, B. D. Cuevas, K. Nakamura, and G. L. Johnson.** 2004. Wiring diagrams of MAPK regulation by MEKK1, 2, and 3. Biochem. Cell Biol. **82:**658–663.
29. **Uhlik, M. T., A. N. Abell, N. L. Johnson, W. Sun, B. D. Cuevas, K. E. Lobel-Rice, E. A. Horne, M. L. Dell'Acqua, and G. L. Johnson.** 2003. Rac-MEKK3-MKK3 scaffolding for p38 MAPK activation during hyperosmotic shock. Nat. Cell Biol. **5:**1104–1110.
30. **Watson, F. L., H. M. Heerssen, A. Bhattacharyya, L. Klesse, M. Z. Lin, and R. A. Segal.** 2001. Neurotrophins use the Erk5 pathway to mediate a retrograde survival response. Nat. Neurosci. **4:**981–988.
31. **Wilson, M. I., D. J. Gill, O. Perisic, M. T. Quinn, and R. L. Williams.** 2003. PB1 domain-mediated heterodimerization in NADPH oxidase and signaling complexes of atypical protein kinase C with Par6 and p62. Mol. Cell **12:**39–50.
32. **Yan, L., J. Carr, P. R. Ashby, V. Murry-Tait, C. Thompson, and J. S. Arthur.** 2003. Knockout of ERK5 causes multiple defects in placental and embryonic development. BMC Dev. Biol. **3:**11–31.
33. **Yun, M., L. Keshvara, C. G. Park, Y. M. Zhang, J. B. Dickerson, J. Zheng, C. O. Rock, T. Curran, and H. W. Park.** 2003. Crystal structures of the Dab homology domains of mouse disabled 1 and 2. J. Biol. Chem. **278:**36572–36581.
34. **Zhou, G., Z. Q. Bao, and J. E. Dixon.** 1995. Components of a new human protein kinase signal transduction pathway. J. Biol. Chem. **270:**12665–12669.